

Investigation on Corona Discharge Parameters at Various Temperatures in Precipitator Electrostatic

M. AISSOU^{1,2}, H. AIT SAID^{1,3}, N. HEBBAR², K. LAIFAOU¹, H. NOURI^{1,4}

¹Laboratoire de Génie Electrique, University A-Mira of Bejaia 06000 Algeria

²Electrical Engineering Department, University Belhadj Bouchaib of Ain Temouchent 46000 Algeria

³Electrical Engineering Department, University Ahmed Zabana of Relizane 48000 Algeria

⁴Electrical Engineering Department, University of Setif_1 19000 Algeria

Email : aissoumass@gmail.com

Abstract - In blade-to-plane electrostatic precipitators at variable temperatures, the electric field and the current density distributions of the negative DC corona were experimentally analyzed, and the corona discharge was used as the source of ionization. In this research, an experimental cell was designed and built to adjust the temperature from 20°C to 46°C within the cell. The current density-voltage characteristic and the radial distance distribution of the current density of an electrostatic blade-to-plane precipitator were measured over a temperature interval. Based on the Tassicker and Townsend models, the electric field and the onset voltage were determined. With the rise in temperature, the corona current obtained at the collector plate has been observed to increase, but the onset voltage decreased. The applied voltage and temperature greatly affected the corona current density characteristics and the electrical field. If an exponent of 4.6 to 5 for a negative corona discharge is taken, the DC density distribution is satisfied, then the current density distribution follows the well-known Warburg theorem.

Keywords - Corona Discharge, current density, Precipitator Electrostatic, Electric field

I. INTRODUCTION

Electrostatic precipitators are widely used for the elimination of fine particles such as dust and smoke from gas in various industrial systems [1-4]. The performance of electrostatic precipitators is influenced by the negative DC corona discharge characteristics. This corona discharge is a phenomenon of an electrical discharge in gasses and is affected by various parameters [5, 6], including temperature, pressure and humidity [7-8]. Various investigations were performed to understand the impact of the temperature on the corona discharge in a blade-to-plane electrostatic precipitator.

Temperature has a significant impact on the corona discharge behaviour. An increase in temperature causes a decrease in the corona onset voltage [9]. There was developed a model for estimating the electrical field on the conductors [9, 10]. This theory was based on the action of pressure and temperature.

The corona discharge distribution in non-uniform fields has been analyzed for several years [10, 11]. The effect of atmospheric parameters such as temperature, pressure, and humidity was taken into account in some cases [12-15], but in many cases the

investigation was limited to ambient normal conditions.

Characterization of the DC corona at high and low temperatures is very useful, for example, in : electrostatic precipitators installed in chimneys, or at which the air density decreases with rising temperatures. The temperature of the gases begins to fall as soon as they are released from the generator. If this decreases too much, the water vapor contained in these gases will condensate. The flue external surface temperature is less than 50°C. However, depending on the nature of the powders, the resistivity at the ambient temperature is always one to three orders of magnitude lower than the resistivity at 50°C. A high voltage electrode in most electrostatic precipitators is supplied with a negative voltage to ensure a good charge of the particles, a sufficiently intensive electric field, and to limit breakdowns as much as possible [5, 6, 10]. The evolution of corona discharge in gas is of particular interest, namely the distribution of ion density on the collector plane.

Awareness of the temperature effect is of critical importance in such DC corona discharge systems. Certain features of this influence call for further

research in order to approve a real mathematical modeling of physical phenomena, such as the essential step towards a precise numerical simulation of the electrostatic precipitation system.

The fundamental objective of this research is to study the influence of temperature on negative DC corona discharges used in blade-to-plane electrostatic precipitators, which can vary from low to high states. In particular, the electrical field, current density distribution and current density-voltage characteristics are studied and analyzed.

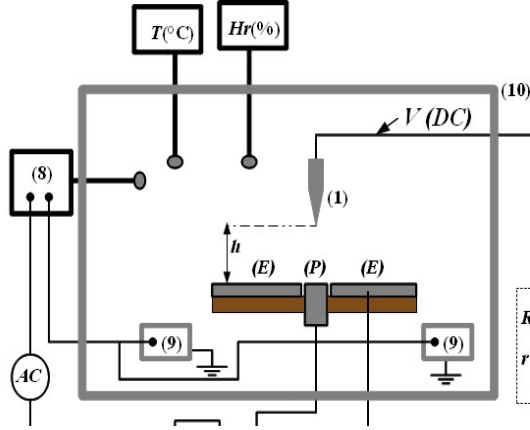


Fig. 1. Experimental Setup.

II. EXPERIMENTAL METHOD

The experimental model of the blade-to-plane electrostatic precipitator used in this study is shown in Figure 1. The high voltage electrode containing the stainless steel blade (1) with a curvature radius of 0.019 mm is fixed with two insulation supports (2). The passive electrodes of the electrostatic precipitator consist of two stainless steel planes (G) and (E), 400 mm-width in y-direction and 800 mm-length in x-direction, respectively. These two electrodes (blade and plane) are spaced $h = 10$ mm apart.

The measurement plane (E) is connected to the ground by means of a current signal resistance of 150 k Ω and the guard electrodes (G) are connected directly to the ground. The air gap between the guard planes (G) and the plane (E) at 0.5 mm is mandatory in order to ensure continuity of field distributions and current at the extremities of (E). Passive electrodes are fastened with insulating screws and the waste current between the high voltage blade and the measuring plane (E) is discharged to the ground by the guard planes (G).

The high voltage applied to the corona blade is supplied by a 0 to ± 140 kV source (5). The DC digital voltmeter (6) and the high voltage divider (7) are used to measure the applied voltage. The bias plane (E) is connected to the DC low voltage source

(4) and the collector probe (P) is connected to the digital multimeter (3). The Ha(g/m³) humidity and T($^{\circ}$ C) temperature measuring devices and the electrode system are mounted in a 200 liter plexiglass case (10). The temperature is controlled by the controller (8) and connected online to the low voltage AC source. Air in the plexiglass box is heated by heating resistors (9).

Tassicker method to determine the electric field under space charge

The authors of [5, 16, 17] have developed a circular bias probe theory, which will be quickly reviewed. The corona discharge current I_0 is captured by the probe collector (P). This corona current will increase or decrease once the voltage V_b is applied to the plane (E) when the electrical field E_b is produced. When the probe collector is placed under the negative corona blade, E_b is added to E when $V_b < 0$ and E_b is opposed to E as $V_b > 0$. On the other hand, when the probe collector (P) is located below the positive corona blade, E_b is opposed to the unknown field E on the probe surface once $V_b < 0$ and E_b is added to E as $V_b > 0$. The corona current discharge I beneath condition V_b and I_0 beneath condition $V_b = 0$ are developed as follows:

$$I = J \times S = \mu \times \rho \times (E + E_b) \times S = \mu \times \rho \times \left(\frac{\varphi_{S0} + \varphi_{SI}}{\varepsilon_0} \right) \quad (1)$$

$$I_0 = J_0 \times S = \mu \times \rho \times E \times S = \mu \times \rho \times \frac{\varphi_{S0}}{\varepsilon_0} \quad (2)$$

$$\varphi_{S0} = S \times E \times \varepsilon_0 \quad (3)$$

$$\varphi_{SI} = C_0 \times V_b \quad (4)$$

$$C_0 = 4r \times \varepsilon_0 \left[1.07944 + 0.5 \times \ln \left(1 + \frac{r}{2g} \right) \right] \quad (5)$$

$$\frac{I}{I_0} = 1 + \frac{C_0}{\pi \times \varepsilon_0 \times r_m^2} \times \frac{V_b}{E} \quad (6)$$

$$\frac{I}{I_0} = 1 + P V_b \quad (7)$$

$$P = \frac{C_0}{\pi \times \varepsilon_0 \times r_m^2 \times E} = \frac{1585.35}{E} \quad (8)$$

where p is the mobility of the ions (m²/V.s), J is the corona current density (A/m), ρ is the space charge density (C/m³), φ_{S0} (Wb) is the flux due to the unknown electric field E (kV/m) to be measured, and φ_{SI} (Wb) is the flux due to the bias electric field E_b (kV/m). C_0 (pF) is the capacity between the bias plane (E) and the probe electrode (P) given by [5], where r (mm) is the collector radius (P) and g (mm) is the air space between (P) and (E), $S = \pi r_m^2$ (m²) is the collector effective surface (P) with r_m (mm) the

effective radius. From equations (3), (4), (5), and (6), the current ratio is given as in [5, 16, 17].

The corona current measurements I_0 and I determine the unknown external field E . The expression (6) gives a linear characteristic of I/I_0 with a bias voltage V_b . However, in the case of high values of V_b , when the total field at the collector surface is opposed, due to the bias of the electrical field $E_b > E$, a deviation of the characteristics occurs, and therefore the expression (6) is not valid. The models of the probe are mainly concerned with the choice of these dimensions and the precision of its construction. The well-sensitivity of the current ratio I/I_0 is obtained for a very small air space g , and the radius of the collector probe r is not very high. The r/g ratio must be as high as reasonably possible. The probe must be moved easily for regular dust purification. The probe electrode radius is $r = 2.235$ mm, the plane orifice is $r_e = 2.27$ mm, giving an air space $g = 0.035$ mm, a ratio $r/g = 64$, the probe electrode an effective radius $r_m = r + g/2$ and a capacity value of $C_0 = 0.223$ pF. The relationship (8) is shown as in [5, 16].

The slope P is determined by the measurements of the current ratio I/I_0 and the bias voltage V_b , the electric field E if P is considered here. A polished blade we used to check the operation of the probe.

The measurements of I/I_0 were carried out at different voltages V_b , between $(-80$ V) and $(+80$ V), where the temperature T and the applied voltage V were kept constant during the tests. The experimental measurements allowed to calculate field E on the collector plane using equations (7) and (8). In all cases, the $I/I_0 = f(V_b)$ characteristic was linear for $(-80$ V) $< V_b < (+80$ V). The deviation of the characteristics occurred for $V_b > (80$ V) or $V_b < (-80$ V).

These results provide a control of the operation of the probe and the limit of the bias voltage V_b . The collector probe was also used to measure the normal current density J when the probe is unbiased $V_b=0$:

$$J = \frac{I_0}{\pi \times r_m^2} \quad (9)$$

where I_0 is the current collected from the corona discharge and the effective radius of the probe is $r_m = 2.25$ mm.

III. RESULTS AND DISCUSSION

In the following sections, the temperature impact on the electrical field, the current density distribution and the current density-voltage characteristics of the passive electrode with a bias probe are discussed. The probe current (I) along the x-position and the y-

position on the collector plane is achieved by displacing the active electrode.

Experimental measurements are performed for different parameters, such as: temperature (T), position (x) of the probe on the plane, applied voltage (V), and the y-axis position is fixed for $h = 40$ mm.

A) Current Density-Voltage Characteristics

The corona discharge characteristics of an electrostatic precipitator are affected by temperature as the electrical field and the ion concentration power play a crucial role in the charging of the particles [18, 19]. In [20], the researchers consider that negative ions are unstable at atmospheric pressures and temperatures in the discharge area where a large number of free electrons are released and sparking easily occurs even under a low applied voltage. The authors of [21] and [22] have stated that the ionization rate of the gas particles can significantly influence the electrostatic precipitation performance at different temperatures and that thermal ionization at very high temperatures should be envisaged [23].

The current density-voltage characteristics of the blade-to-plane electrostatic precipitator at different temperatures are shown in Figure 2.

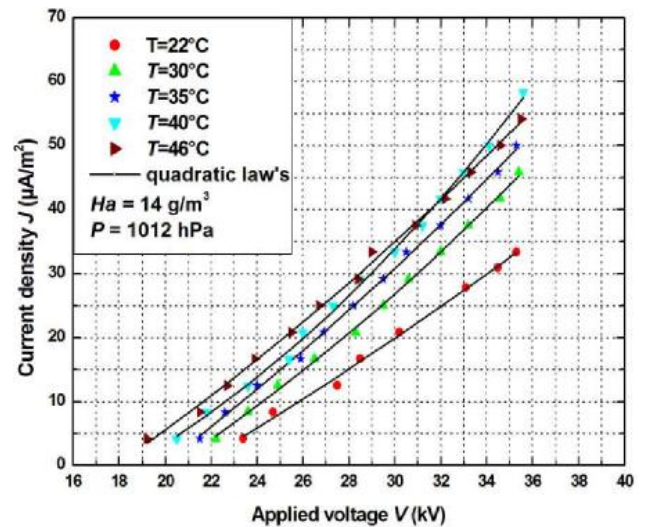


Fig. 2. Current density-voltage characteristics, $V_b = 0$.

The corona discharge current density (J) is a quadratic function with the applied voltage (V). Depending on the voltage applied, the temperature influence of the DC corona discharge current is different. The electrical operating point at the blade-to-plane electrostatic precipitator is the values of voltage and current at which the precipitator operates. Because of the importance of temperature in the electrical characteristics, $J = f(V)$ curves are

plotted in Figure 2 for different values of temperature.

The plots illustrate that the current density level increases at the same applied voltage, but the corona onset voltage decreases as temperature increases due to the fact that the mean free path of ions increases with temperature. The authors in [24] and [25] have developed a simple theoretical formula on the relationship between the corona current and the applied voltage in a wire-to-cylinder geometric system, and the low current empirical law for the wire-to-plane configuration was derived in [6].

Afterwards, it was experimentally observed that the Townsend formula could also be used approximately for blade-to-plane configuration, as demonstrated in [10]. The law can be given as :

$$I = K \times V \times (V - V_0) \quad (10)$$

$$J = \frac{K}{S} \times V \times (V - V_0) \quad (11)$$

were K is a dimensional constant depending on the blade electrode radius, the charge carrier mobility in the drift region, the inter-electrode gap, and other geometrical parameters.

Figure 2 shows that the corona current at the probe region increases with the temperature rise. During the growth of the gas temperature, the electrons acquired more energy for forming an avalanche, and the average free path of gas molecules increased.

For the applied voltages greater than 32 kV (close to the breakdown voltage), the corona discharge had a large number of streamers in its ionization zone, this explains this excess of speed generated in the blade electrode by the fact that the streamers also induce the electric wind.

It is generally accepted that due to the presence of the ionic wind or the difference in velocities between ions and charged particles the rate of turbulence increases. An increase in temperature to 46°C decreased the rate of turbulence and increased the resistivity of the particles.

B) Assessment of the Regression Model Relevance

The estimation of the curve model consists of two characteristics : the summary of the model and the estimation of the parameter presented in Table 1.

In this Table, the model summary provides the regression coefficient (R), the statistic (F) being the ratio of the regression mean squares (inter group) and the residual mean squares (intra group); the freedom degrees ($df1$, $df2$, and $Sig.$) indicate whether the test is significant or not, and the parameter estimates provide the quadratic equations parameters (b_0 , b_1 , and b_2).

The F , $df1$, $df2$, and $Sig.$ columns summarize the results of the F test of the model fit. The significance value of the F statistic is less than 0.05%, which means that the variation explained by each model is not random. The R^2 statistic is a better measure of the strength of relationship. The quadratic law is a model whose equation is $J = b_0 + b_1 V + b_2 V^2$ (A/m²). The quadratic model can be used to model a series that starts off or a series that dampens.

In order to be relevant to the model, the improvement obtained with the independent variable must be large, and the residuals between the observed values and the regression shall be small. To test this, this model proceeds with the F value test. The value of F was calculated automatically, and the associated level of significance can be found in the last column of the model summary [26, 27].

The F value is greater than 600 and is significant at $m < 0.0005$. This means that the probability of obtaining an F value of this size by chance is less than 0.05%. Therefore, there is a statistically significant relationship between the dependent variable J (A/m²) and the independent variable V (kV). It can therefore be concluded that the model with a predictor makes it possible to predict the variable (J) better than the model without a predictor [27, 28].

C) Evaluating Data Fit to the Regression Model

If there is a significant improvement in the model, it is necessary to report to what extent the data is fitted to this model. In a way, it is possible to quantify how well the pattern represents the dispersion of the points in the graph.

This information can be found in Table 1, with index (R) showing the value of the multiple model correlation. The multiple correlation (R) is interpreted as a simple correlation. It represents the combined correlation between all independent variables of the model and the dependent variable. Since there is only one independent variable here, this coefficient is the same (in the absolute value) as the correlation coefficient as mentioned in [26, 29, 30].

The value of the multiple correlation coefficient in Table 1 is greater than 0.998. This value indicates that the data are very well suited to the model and can be found in the column (R^2). If the coefficient of correlation is squared, it will give an R^2 value greater than 0.996.

This shows the proportion of the variability of the dependent variable (J) explained in the regression model.

Table 1. Model summary and parameter estimates with dependent variable: corona current density J ($\mu\text{A}/\text{m}^2$) and independent variable: applied voltage V (kV).

Equation	Model Summary					Parameter	
	R ²	F	df1	df2	Sig.	b_0	
T=22°C	Quadratic	0.996	599.846	2	5	0.000	-38.027
T=30°C	Quadratic	0.999	2952.453	2	8	0.000	-30.954
T=35°C	Quadratic	0.999	3296.810	2	9	0.000	-42.371
T=40°C	Quadratic	0.998	2382.017	2	10	0.000	-11.703

D) Onset of Corona Discharge

The onset voltage of the corona discharge is the applied voltage required to arrive at the critical electrical field necessary for the ionization of the air molecules that close the blade surface. Peek' formula [31] connects this onset voltage to the disruptive critical potential gradient as a function of inter-electrode distance $h = 40$ mm, $r_c = 0.019$ mm radius curvature, (T) temperature and (P) gas pressure :

$$V_0 = m_v \times g_0 \times \delta^2 \times r_c \times \left(1 + \frac{0.0308}{\sqrt{\delta \times r_c}} \right) \ln \left(\frac{2 \times h}{r_c} \right) \quad (12)$$

$$\delta = \frac{3.92 \times P}{273 + T} \quad (13)$$

The δ parameter is a gas density factor that is based on the temperature and pressure. Temperature T in degrees celsius ($^{\circ}\text{C}$) and pressure P in centimeters of mercury (cmHg). At standard temperature and pressure $\delta = 1$. The condition of the wire is presented by the factor m_v , irregularity, the curvature radius wire r_c and the inter-electrode gap h . Depending on the wire condition, m_v varies from 0.85 to 0.98 and $m_v = 1$ for ideal smooth wires. The disruptive critical potential gradient g_0 is on the order of 30 kV/cm or 27.2 kV/cm for air [32].

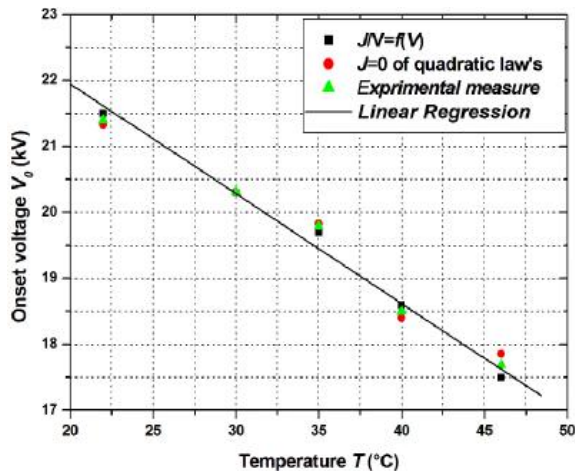


Fig. 3. Onset voltage with temperature.

The effect of temperature on corona discharge is shown in Figure 3. The illustrations $(J/V) = f(V)$ and $J = 0$ of the quadratic law's are chosen here to indicate the corona discharge onset. The corona onset voltage decreases with the increase of the temperature when more heat is added to the system, the coefficient of attachment (η) and the coefficient of ionization (α) both increase so that the increase of the attachment coefficient is lower than that of the ionization coefficient, so that the increase of the temperature causes the increase of the effective ionization coefficient ($\alpha \cdot \eta$). These factors have contributed to a decrease in corona onset voltage with an increase in temperature, so that the onset voltage decreases at a high gas temperature, in accordance with the provisions of the Peek law [31]. The linear regression model shown in Figure 3 is as follows:

$$V_0 = A + B \times T \quad (13)$$

The non-standardized coefficients allow reconstructing the regression line equation. The intercept is the value $A = 25.279$ kV of the constant in the equation, and the slope is indicated by the value $B = -0.167$ kV/ $^{\circ}\text{C}$ of the independent variable, with $R = -0.995$ and $m = 0.000265 < 0.0005$. However, the value of the correlation coefficient (R) provides new information: the sign of that value: + or -. It is important to know this value in order to interpret the meaning of the relationship between the dependent and the independent variables. Consequently, the current value of the coefficient is $R = -0.995$, taking into account the negative relationship between the two variables. The last coefficient indicates that the regression model fits the data very well.

E) Current Density Distributions of the Passive Electrode

The ionic current-density distribution on the collector is an aspect of the DC corona discharge in air, which is of a particular interest in the case of a blade-to-plane electrostatic precipitator. In the experiments here, it was found showed that this distribution under the following relationship corresponds to Warburg's law as stated in [10] :

$$J(x) = J(\theta) = J(0) \cos \theta^P \quad (14)$$

where θ is a distribution angle relative to the hypotenuse between the electrodes, both the discharge blade (z -axis) and the probe on the collection plate (x -axis). $J(0)$ refers to the current density of the corona directly under the discharge blade.

The collection efficiency varies along the collector plane length in proportion to the amount of the

collector current at that collector location, as shown in Figures 4 and 5. The maximum collection efficiency occurs within a specified collector plane at collector locations facing the corona blade electrode, where collector currents are at their maximum value each of which follows the Warburg collector current distribution for different maximum collection efficiencies at different maximum collector currents. It is possible to estimate the amount of dust collected along the collector plane. Estimates of dust collected with the maximum collection efficiencies were of 95% (to $x = 0$ mm) and 0% (to $x = 60$ mm), all with the Warburg collector current distribution.

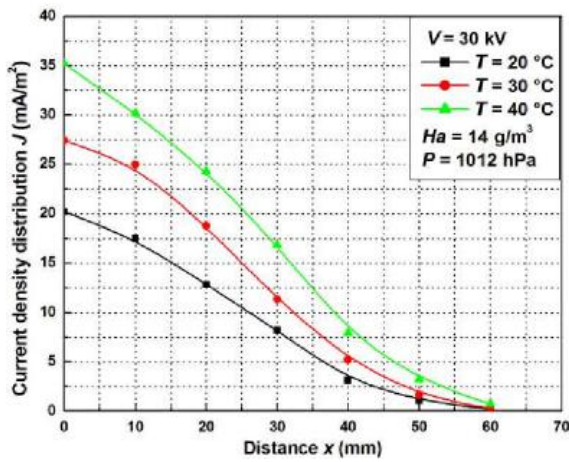


Fig. 4. Current density distribution with radial distance, $V = 30$ kV.

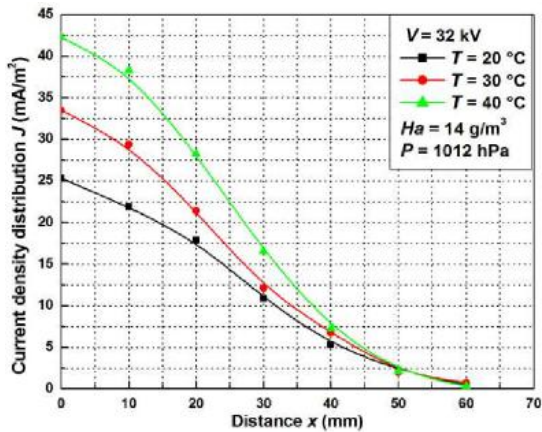


Fig. 5. Current density distributions with radial distance, $V = 32$ kV.

The exponent value p varies depending on the temperature and the applied voltage. Warburg found a p value of 4.5 to 5 for negative polarities [10], and it was not possible to round the exponent to a 5.0 value because it is an abnormal practice. The Warburg distribution is confirmed by Figures 4 and 5. The corona current density distribution agrees well with the Warburg relationship, provided that the exponent is taken as $p=5$ and $p=4.9$ for the applied voltage $V=32$ kV, and $V=30$ kV, respectively.

The values 4.7, 4.9, and 4.6 in Figure 6 and the exponent p in Figure 7 are well suited to the experimental results. It should be noted that in a DC monopolar corona [12], where the probe collector is fixed at the center of the plane collector beneath the high voltage electrode, the values of J and E are at a maximum for $x=0$, and they decrease at the movements away from the centre of this plane along the x -axis according to the Warburg law.

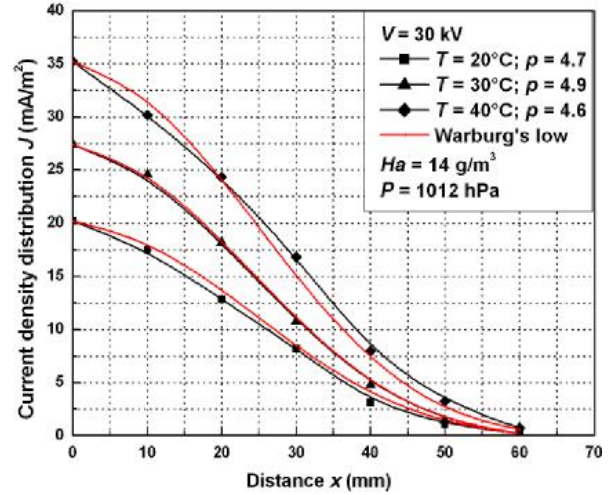
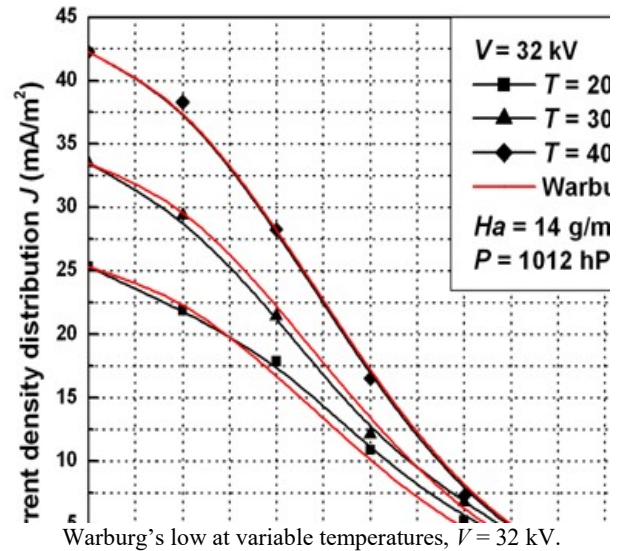


Fig. 6. Current density distributions with radial distance and Warburg's law at variable temperatures, $V = 30$ kV.



F) Current Density and Electric Field

Figures 8 and 9 show the experimental results of the measured current density (J) and the electrical field (E) at the probe collector, depending on the temperature (T) with different corona applied voltage (V), and the mutual approximation of the current density assumes that the current density is simply proportional to the electrical field. They show how the configuration of the electrical field changes with the gas temperature between the two electrodes. It can be seen that at a temperature of 20° C, field lines are mostly attracted by the additional ground potential boundary, while at 40° C more lines terminate on the collector surface.

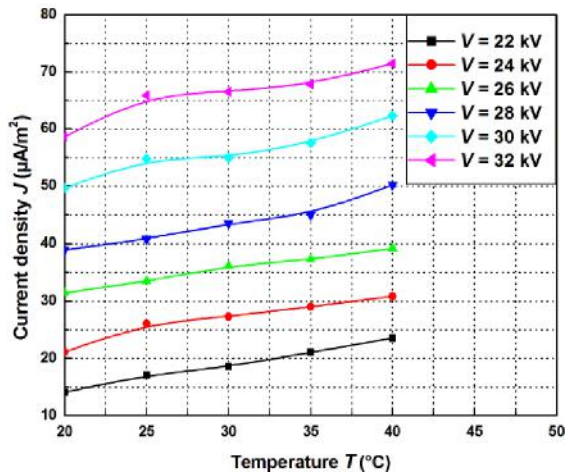


Fig. 8. Measured current density vs. applied voltage for various temperatures at $V_b = -60\text{V}$, $h = 40\text{ mm}$, $H_a = 14\text{g/m}^3$ and $P = 1012\text{ hPa}$.

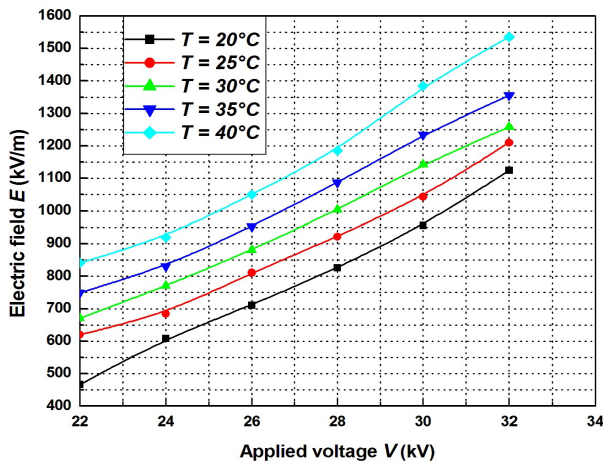


Fig. 9. Electric field vs. applied voltage for various temperatures at $h = 40\text{ mm}$, $H_a = 14\text{g/m}^3$ and $P = 1012\text{ hPa}$.

Figure 8 shows the increase in current density with an increase in temperature at different applied voltages. A few electrons move straight to the collector plane, without being blocked by gas molecules, to generate an electron carrying current when the temperature is above 20°C . The electron current increases with the growth of the applied voltage and the gas temperature, increasing to $72\ \mu\text{A/m}^2$ below the applied voltage of 22 kV and to a temperature of 40°C . Electric field measurements influenced by space charge are of key importance for the analysis of corona discharge characteristics and the ion flow field in corona discharge applications such as electrostatic precipitators.

Tassicker suggested a boundary bias probe process to establish the electrical field strength at the probe surface of the collector electrode with the existence of a space charge.

Figure 9 shows the electrical field strength on the surface of the probe collector with respect to the different temperature at the applied voltage V . The field is very unevenly distributed at different temperatures. The degree of irregularity is between 20°C and 40°C . The electrical

field tends to the Laplacian field at low voltage, but breakdown happens at high applied voltage when the field E is near the propagation field; $E = 1100\text{ kV/m}$ is required for the negative streamer at $T = 20^\circ\text{C}$. The field also grows with the applied voltage at a given temperature. In this configuration system, the electrical field can reach up to $E = 1550\text{ kV/m}$ for very high temperatures and high voltages.

The most important change is the large increase in the electrons number in the collector region. Additional electrons are generated in two ways:

- ✓ Accelerate the electron detachment of negative ions in the collector region by increasing the temperature of the gas.

- ✓ Confirm by generating energetic electrons directly with enhanced secondary ionization or cathode thermal emission at elevated temperatures. The electrons are accelerating to the collector planes, and the corona discharge current is becoming an even greater current. The airflow acceleration known as ionic wind is caused by a momentum transfer during collisions. The action-reaction principle causes a force to be exerted on the electrodes, which is known as electro hydrodynamic thrust. When the applied voltage approaches the breakdown voltage, the electric wind influences the experimental measurements, leading to a hypothesis of a possible involvement of streamers in the mechanism of electric wind generation, in addition to the role of ions. The discharge does, in fact, have a large number of streamers in its ionization zone. Perhaps an extra speed generated by the discharge in the axis of the high voltage electrode can be explained by the fact that the streamers also induce the electric wind. The presence of the ionic wind or a difference in velocities between ions and charged particles within blade-to-plane electrostatic precipitator is thought to reduce the collection efficiency by increasing the rate of turbulence.

IV. CONCLUSION

In this article, we revealed the negative characteristics of DC corona discharge in an electrostatic precipitator blade-plane configuration system at various temperatures from 22°C to 46°C . Current density distributions, current density and electric field are measured in an electrostatic precipitator with varying temperatures, supporting a bias probe on the ground plane. A typical Townsend quadratic law is followed by the current evolution versus applied voltage. By increasing temperature at a given voltage value, it is considerably increased and decreased with 32 kV , $T = 46^\circ\text{C}$. The onset of the corona effect decreased by increasing temperature, which was in line with the Peek model prediction. The linear regression parameters and the quadratic law of the models imply that the regression models match the data very well.

The Warburg law is equivalent to the measured current density distributions, according to the superimposing theorem. The electrical conductivity of gas increased because the electric field increases linearly with the applied voltage and temperature.

References

- [1] Mizuno, A., Electrostatic precipitation. *IEEE Trans. Dielectr. Electr. Insul.*, 2000, vol. 7, no. 5, pp. 615-624.
- [2] Fujishima, H., Morita, Y., Okubo, M., Yamamoto, T., Numerical simulation of three-dimensional electrohydrodynamics of spiked-electrode electrostatic precipitators, *IEEE Trans. Dielectr. Electr. Insul.*, 2006, vol. 13, no. 1, pp.160-167.
- [3] Jaworek A., Krupa A., Czech T., Modern electrostatic devices and methods for exhaust gas cleaning: A brief review, *J. Electrosta.*, 2007, vol. 65, no. 3, pp.133-155.
- [4] Chang, J., S., Next generation integrated electrostatic gas cleaning systems, *J. Electrosta.*, 2003, vol. 57, no. 3-4, pp. 273-291.
- [5] Ait Said, H., Nouri, H., Zebboudj, Y., Effect of air flow on corona discharge in wire-to-plate electrostatic precipitator, *J. Electrosta.*, 2015, vol. 73, no. 1, pp.19-25.
- [6] Ait Said, H., Nouri H., Zebboudj, Y., Analysis of current-voltage characteristics in the wires-to-planes geometry during corona discharge, *Eur. Phys. J. AP*, 2014, vol. 67, no. 3, p. 30802.
- [7] Podlinski, J., Niewulis, A., Mizeraczyk, J., Electrohydrodynamic flow and particle collection efficiency of a spike-plate type electrostatic precipitator, *J. Electrosta.*, 2009, vol. 67, no. 2-3, pp. 99-104.
- [8] Wang, X., You, C., Effect of humidity on negative corona discharge of electrostatic precipitators, *IEEE Trans. Dielectr. Electr. Insul.*, 2013, vol. 20, no. 2-3, pp. 1720-1726.
- [9] Patiño, D., Crespo, B., Porteiro, J., Villaravid, E., Granada, E., Experimental study of a tubular-type ESP for small-scale biomass boilers. Preliminary results in a diesel engine, *Powder Technol.*, 2016, vol. 288, no. 2, pp. 164–175.
- [10] Kaci, M., Ait Said, H., Laifaoui, A., Aissou, A., Nouri, H., Zebboudj, Y., Investigation on the corona discharge in blade-to-plane electrode configuration, *Braz. J. Phys.*, 2015, vol. 45, no. 6, pp. 643–655.
- [11] Robledo-Martinez, A., Characteristics of DC corona discharge in humid, reduced-density air, *J. Electrosta.*, 1993, vol. 29, no. 2, pp. 101-111.
- [12] Aissou, M., Ait Said, H., Nouri, H., Zebboudj, Y., Analysis of current density and electric field beneath a bipolar DC wires-to-plane corona discharge in humid air, *Eur. Phys. J. AP*, 2013, vol. 61, no. 3, p. 30803.
- [13] Nouri, H., Zouzou, N., Moreau, E., Dascalescu, L., Zebboudj, Y., Effect of relative humidity on current-voltage characteristics of an electrostatic precipitator, *J. Electrosta.*, 2012, vol. 70, no. 1, pp. 20-24.
- [14] Nouri H., Aissou M., Zebboudj Y., Modeling and simulation of the effect of pressure on the corona discharge for wire-plan configuration, *IEEE Trans. Dielectr. Electr. Insul.*, 2013, vol. 20, no. 5, pp. 1547-1553.
- [15] Ait Said, H., Aissou, A., Nouri, H., Zebboudj, Y., Analysis of the current–voltage characteristic during the corona discharge in wires-to-planes electrostatic precipitator under variable air humidity. *Acta Phys. Pol. A*, 2019, vol. 135, no. 3, pp. 320-325.
- [16] Nouri, H., Zebboudj, Y., Analysis of positive corona in wire-to-plate electrostatic precipitator, *Eur. Phys. J. AP*, 2010, vol. 49, no. 1, p.11001.
- [17] Tong, Y., Lin, L., Zhang, L., Bu, S., Chen, F., Shao, W., Feng, C., Weigang Xu, Qi, Q., Fu, L., Separation of fine particulates using a honeycomb tube electrostatic precipitator equipped with arista electrodes, *Sep. Purif. Technol.*, 2020, vol. 236, no 4, p. 116299.
- [18] Mizuno, A., Electrostatic precipitation, *IEEE Trans. Dielectr. Electr. Insul.*, 2000, vol. 7, no. 5, pp. 615-624.
- [19] Darcovich, K., Jonasson, K., A., Capes, C., E., Developments in the control of fine particulate air emissions, *Adv. Powder Technol.*, 1997, vol. 8, no. 3, pp.179-215.
- [20] Fasoli, M., Vedda, A., Mihokova, E., Nikl, M., Optical methods for the evaluation of the thermal ionization barrier of lanthanide excited states in luminescent materials, *Phys. Rev. B*, 2012, vol. 85, no. 8, pp. 85-127.
- [21] Shale, C., C., Progress in high-temperature electrostatic precipitation, *J. Air Pol. Contr. Assoc.*, 1967, vol. 17, no. 3, pp. 159-160.
- [22] Shale, C., C., Holden, J., The role of wire size in negative electrical discharge at high temperature. Industry and General Applications, *IEEE Trans. Ind. Gen. Appl.*, 1969, vol. 5, no. 1, pp. 34-39.
- [23] Cooperman, P., Spontaneous ionization of gases at high temperature, *IEEE Trans. Ind. Appl.*, 1974, vol. 10, no. 6, pp. 520-523.
- [24] Yala, H., Zebboudj, Y., Finite-element solution of monopolar corona in a coaxial system, *Eur. Phys. J. AP*, 2002, vol. 19, no. 2, pp. 123-129.
- [25] Conesa A., J., Sánchez, M., The current–voltage characteristics of corona discharge in wire to cylinder in parallel electrode arrangement, *IEEE Trans. Plas. Sc.*, 2018, vol. 46, no. 8, pp. 3022-3030.
- [26] Weisberg S., *Applied Linear Regression*, New Jersey : Wiley, 2014.
- [27] Cohen J., *Statistical Power Analysis for the Behavioral Sciences*, New York : Lawrence Erlbaum Associates, 1988.
- [28] Tenenhaus, M., *Statistique Méthodes pour Décrire, Expliquer et Prévoir*, France : Dunod, 2007.
- [29] Dodge, Y., Rousson, V., *Analyse de régression appliquée*, France : Dunod, 2004.
- [30] Johnston, J., Dinardo, J., *Méthodes Économétriques*, France : Economica, 1999.
- [31] Guo, B.,Y., Guo, J., Yu, A., B., Simulation of the electric field in wire-plate type electrostatic precipitators, *J. Electrosta.*, 2014, vol. 72, no. 4, pp. 301-310.
- [32] Meng, X., Zhang, H., Zhu, J., A general empirical formula of current–voltage characteristics for point-

to-plane geometry corona discharges, *J. Phys. D Appl. Phys.*, 2008, vol. 41, no. 6, p. 065209.

Author address :

AISSOU Massinissa (Electrical Engineering
Department, University of Ain Temouchent, Algeria, BP
46000 Ain Temouchent, Algeria),
Email: aioumass@gmail.com